J Appl Electrochem (2015) 45:169–176
DOI 10.1007/s10800-014-0778-8

RESEARCH ARTICLE

Physical and electrochemical characteristics of carbon content in carbon-coated Li_2MnSiO_4 for rechargeable lithium batteries

Sora Won · Kyung-Koo Lee · Gyungse Park · Ho-Jung Sun · Jung-Chul An · Joongpyo Shim

Received: 25 August 2014 / Accepted: 10 November 2014 / Published online: 23 November 2014

Abstract Carbon-coated Li_2MnSiO_4 powders were synthesized by a citric acid-assisted sol–gel process, and their physical and electrochemical properties were characterized to assess their suitability as a cathode material in lithium-rechargeable batteries. Carbon was coated onto the Li_2MnSiO_4 particles through the carbonization of polymeric materials that were caused by the addition of citric acid during the sol–gel process. The particle size and electrical conductivity of the Li_2MnSiO_4 powders were found to be changed by varying the amount of citric acid added during the sol–gel process. XRD analysis showed that the quantity of impurities in Li_2MnSiO_4 was decreased during the sol–gel process. The carbon coating led to an increase in conductivity and mean particle size by creating an electrical and physical connection between the particles. The discharge capacity of Li_2MnSiO_4 with over 5 % carbon coating was significantly increased to $\sim$125 mAh g^{-1} compared to just $\sim$3 mAh g^{-1} for noncoated material.

S. Won · J. Shim (✉)
Department of Nano & Chemical Engineering, Kunsan National University, Gunsan, Jeonbuk 573-701, Korea
e-mail: jpshim@kunsan.ac.kr

K.-K. Lee · G. Park
Department of Chemistry, Kunsan National University, Gunsan, Jeonbuk 573-701, Korea

H.-J. Sun
Department of Material Science & Engineering, Kunsan National University, Gunsan, Jeonbuk 573-701, Korea

J.-C. An
Carbon Materials Research Group, Research Institute of Industrial Science & Technology, Pohang, Gyeongbuk 790-330, Korea

Keywords Li_2MnSiO_4 · Sol–gel process · Cathode · Lithium ion battery

1 Introduction

The extraction/insertion of lithium in polyanion frame works, for example, $(XO_4)^{n-}$ materials (where X = P, S or Si), has been intensively studied ever since the Goodenough group first reported about their electrochemical properties [1–3]. In particular, $LiFePO_4$ has been intensively studied as a possible substitutional material for commercially available $LiCoO_2$; however, its redox voltage and theoretical capacity have been limited to $\sim$3.5 V and 170 mAh g^{-1}, respectively. As an alternative, Li_2MnSiO_4 is a very promising candidate to replace $LiCoO_2$ as a cathode material in lithium-rechargeable batteries because of its high theoretical capacity of 333 mAh g^{-1} [4]. Furthermore, the Mn redox couple (Mn^{2+}/Mn^{4+}) is of particular interest due to its high potential (vs. Li/Li^+), as well as it being a more plentiful and environmentally friendly resource. Dominko et al. were the first to discover that only 0.6 Li^+ ions could be extracted during the first cycle, whereas 0.3 Li^+ could be reversibly extracted and inserted during the 5th cycle at C/30 rate [5].

The use of Li_2MnSiO_4 as a cathode material in lithium-rechargeable batteries has been limited by its poor electrical conductivity (10^{-14}–10^{-16} S cm^{-1}) [6, 7] which is 4–6 orders of magnitude lower than that of even the poorly conducting $LiFePO_4$ ($\sim 10^{-10}$ S cm^{-1}) [8]. It is, however, well known that the poor conductivity of particles in lithium batteries can be improved simply by applying a carbon coating to their surface [9–11].

Several researchers have previously reported the synthesis of Li_2MnSiO_4 by a sol–gel process [12–14], and a

citric acid-assisted sol–gel process with in situ carbon coating has been proposed by Dominko's [15] and Zhang's [16] groups. More recently, Zhang et al. synthesized in situ carbon-coated Li_2MnSiO_4 using Li and Mn acetates and tetraethyl orthosilicate (TEOS) by means of this citric acid-assisted sol–gel process [17], observing not only an increase in the carbon content but also in the level of impurities, with an increasing amount of citric acid.

In this work, Li_2MnSiO_4 powders with different carbon contents were synthesized by changing the amount of citric acid added during sol–gel synthesis which in many ways is very similar to Zhang's work [16, 17]. Where it differs, however, is that a cheaper and commercially available SiO_2 powder was used as the Si source in place of the TEOS used previously. The effects of changing the carbon content on the structural, morphological, and electrochemical properties of the Li_2MnSiO_4 powders were then investigated in detail and compared against similar results in the literature [17].

2 Experimental

Li_2MnSiO_4 was prepared using a minor variation of a previously described sol–gel process [16, 17], in which lithium acetate (Aldrich), manganese acetate (Aldrich), and fumed silica (SiO_2, 7 nm, Aldrich) were used as precursors with citric acid (Aldrich) as the chelating agent without any further purification. Stoichiometric amounts of all the precursors were first dissolved in deionized water, to which citric acid was added in amounts varying from 0 to 1.25 times the molar content of Li and Mn. The resulting solution was heated at 80 °C for 6 h and then dried at 120 °C for 2 h in order to remove the solvent. The powders obtained were then calcined at 700 °C for 12 h under a nitrogen atmosphere to prevent further oxidation of Mn^{2+} to Mn^{3+} or Mn^{4+} by the oxygen. The carbon content and weight loss during heat treatment was determined by thermal gravimetric analysis (TGA, TA Instrument).

The crystal structures of the samples were identified by X-ray diffraction (XRD, PANalytical, EMPYREAN) with Cu Kα radiation. The sample's morphology and chemical composition were analyzed by a field emission scanning electron microscope (FESEM, Hitachi, S-4800) and a transmission electron microscope (TEM, JEOL, JEM-2010). For conductivity measurement, the powders were pelletized under 5 ton of pressure after mixing with 20 wt% of polyvinylidend fluoride (PVDF, Arkema) as a polymer binder. The apparent electrical conductivity of the pellets was then measured by a four-point probe method using a conductivity meter (Changmin Tech, CMT-SR-100 N).

The electrode for electrochemical testing was prepared from 70 wt% Li_2MnSiO_4, 20 wt% carbon (Super-P) as a conductive agent, and 10 wt% PVDF as a binder. All materials were first mixed in NMP (1-methyl-2-pyrrolidone, Aldrich) for 10 h using a ball-mill, and then cast onto an Al foil current collector (20 μm). The resulting electrodes were dried at 120 °C under vacuum to remove any solvent, and were then stored in an Ar-filled glovebox. Electrochemical measurements were carried out using CR 2032 coin cells (Hoshen) assembled in the glovebox. The electrolyte was 1.0 M $LiPF_6$ in a mixture (1:1:1) of ethylene carbonate (EC), ethyl methyl carbonate (EMC), and dimethyl carbonate (DMC) (Technosemichem). These coin cells were assembled with lithium foil (Aldrich) as the negative electrode and a polypropylene separator (2400, Celgard). The charge and discharge tests were performed at room temperature using a battery cycler (WBCS3000, WonAtech) in the voltage range of 2.0–4.7 V (vs. Li/Li^+).

3 Results and discussion

Li_2MnSiO_4 has three crystal structures, consisting of one monoclinic and two orthorhombic structures [18]. The two orthorhombic phases assigned to the $Pmn2_1$ and $Pmnb$ space groups are isostructural with Li_3PO_4 and Li_2CdSiO_4 prepared at low temperature [19]. On the other hand, the monoclinic structure ($P2_1/n$ space group) is a superlattice of the high-temperature orthorhombic Li_3PO_4. The orthorhombic phases have a 2D layered structure, which was suggested by Politaev et al., to provide greater freedom for the motion of Li^+ ion than the 3D framework of the monoclinic phase [20]. Furthermore, Belharouak et al. reported that Li_2MnSiO_4 contained impurities, such as MnO at 600 °C, Mn_2SiO_4, and Li_2SiO_3 at 800 °C, whereas the samples prepared at 700 °C were of the highest purity [21]. Consequently, the samples used in this study were calcined at 700 °C for 12 h under a nitrogen atmosphere. The XRD patterns obtained for Li_2MnSiO_4 synthesized by the sol–gel process using various amounts of citric acid are shown in Fig. 1. From this figure, it can be seen that the crystal structures of those Li_2MnSiO_4 powders synthesized with citric acid (Fig. 1b–e) were mainly of orthorhombic form, whereas that synthesized without citric acid contained a tiny amount of monoclinic phase (Fig. 1a) [20], which exhibited small peaks at 21.7° and 22.6°. All the samples contained at least some impurities, predominantly Mn_2SiO_4 and MnO, which were inevitable based on previous reports [22–25]. However, the addition of citric acid during calcination dramatically reduced these impurities and the crystallinity of Li_2MnSiO_4, as demonstrated by the reduced intensity of their respective XRD peaks. This is in contrast to Zhang's report, in which the peak intensity of Mn_2SiO_4 decreased with the increasing carbon content but those for MnO and Li_2SiO_4 increased [17]. However, it

should be noted that there have been other reports of the decrease in impurities by carbon coating [13, 26].

The amounts of carbon coated onto the Li_2MnSiO_4 could be simply measured by TGA, as shown in Fig. 2. Since the carbon prepared from organic compounds burns off in air above 300 °C, a weight loss can be clearly observed starting at around 300 °C and finishing at around 430 °C, which is similar to the results reported by Dominko and Zhang et al. [7, 17]. The weight increase observed beyond 570 °C seems to be the result of further oxidation of the Mn by reaction with oxygen. The carbon contents were therefore determined from the weight loss at around 430 °C, which revealed an increase in carbon content with the increasing amount of citric acid. This means that the citric acid was polymerized and coated onto the precursors, and that its derivatives could be converted into carbon materials during calcination [27].

It is well-known that Li_2MnSiO_4 is poorly conductive; Dominko has reported its conductivities at room temperature and 60 °C as being 5×10^{-16} and 3×10^{-14} S cm^{-1}, respectively [7]. Figure 3 shows the electrical conductivities of Li_2MnSiO_4 pellets at room temperature, which were prepared using a PVDF binder (20 %). This demonstrates that the electrical conductivity of noncoated Li_2MnSiO_4 is 3.71×10^{-6} S cm^{-1}, while that of Li_2MnSiO_4 coated with 5.5 % carbon sharply increases to 5.71×10^{-4} S cm^{-1}. Furthermore, the conductivity is increased with the increasing carbon content. These values are significantly higher than those of Dominko's report but very similar to those of Zhang's report [17]. This may be attributable to differences in the pelletizing procedure used.

In Raman spectroscopy, a peak in the range of 1,550–1,660 cm^{-1} is denoted as a graphite band (G-band), which for a carbon material has a high degree of symmetry and an ordered structure. Meanwhile, the bands observed between 1,250 and 1,450 cm^{-1} correspond to a disorder-induced phonon mode (D-band), which has a high intensity in disordered carbon materials [28]. The relative intensities (I_D/I_G) of these D and G bands are therefore directly associated with disorders in the carbon structure [29]. Moreover, Doeff et al. reported that the cell performance of carbon-coated $LiFePO_4$ is dependent on the quantity and quality of the carbon [30]. Figure 4 shows the Raman spectra of the carbon-coated Li_2MnSiO_4, and the relative ratio of I_D and I_G, in which the peaks at ~1,340 and ~1,590 cm^{-1} are assigned to the D and G bands, respectively. The very small peak around 800 cm^{-1} corresponds to the symmetrically stretching internal vibrational modes of SiO_4 anions in Li_2MnSiO_4 [26, 31]. The I_D/I_G ratios of the carbon-coated Li_2MnSiO_4 are in the range of

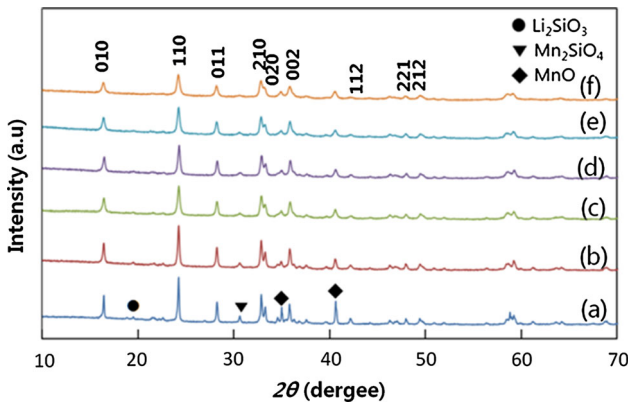

Fig. 1 XRD patterns of Li_2MnSiO_4 for molar ratio of citric acid to metal content. *a* 0, *b* 0.25, *c* 0.5, *d* 0.75, *e* 1.0 and *f* 1.25

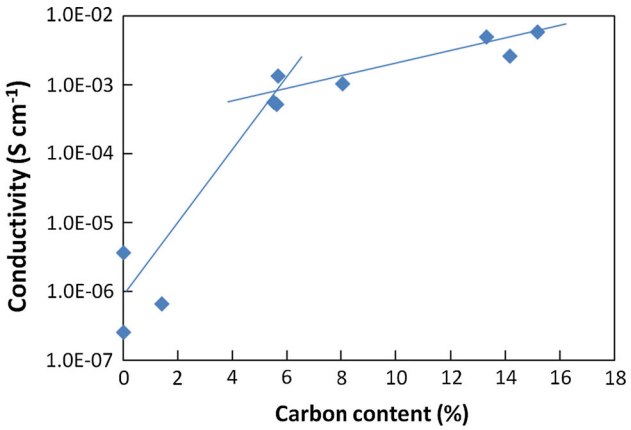

Fig. 3 Variation of electrical conductivity for Li_2MnSiO_4 as a function for carbon content

Fig. 2 TGA **a** of precursors and carbon content **b** of Li_2MnSiO_4 for molar ratio of citric acid to metal content. *a* 0, *b* 0.25, *c* 0.5, *d* 0.75, *e* 1.0, and *f* 1.25

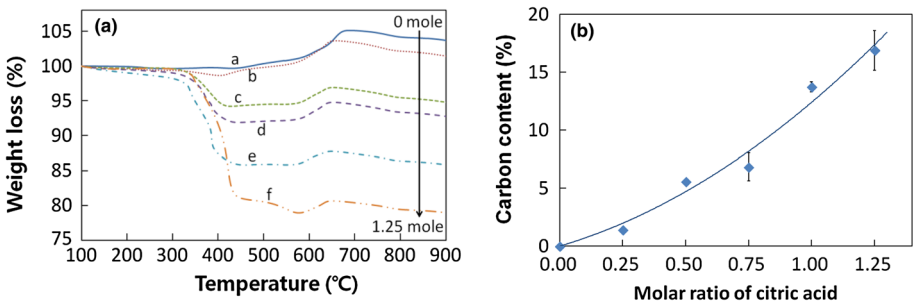

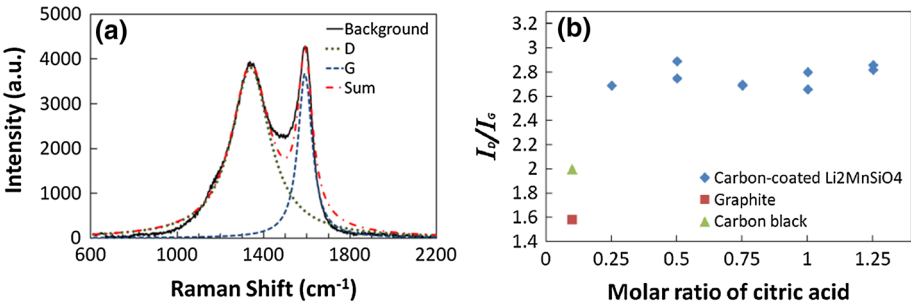

Fig. 4 Raman spectra **a** of carbon-coated Li_2MnSiO_4 powders synthesized at 1.0 mol ratio of citric acid and I_D/I_G intensity ratio **b** for molar ratio of citric acid to metal content

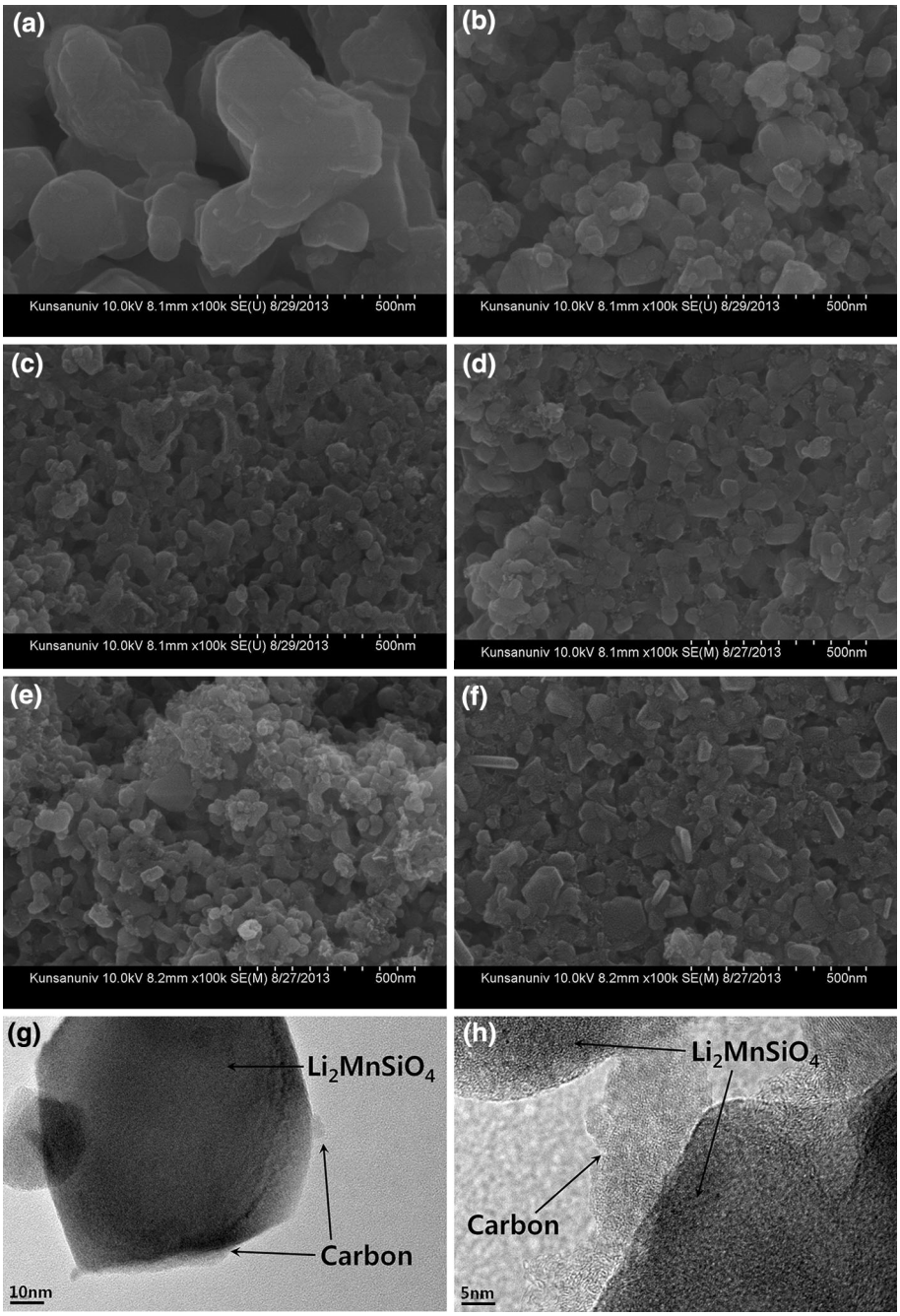

Fig. 5 SEM **a**–**f** and TEM **g**, **h** images of Li_2MnSiO_4 powders. Molar ratio of citric acid to metal content; *a* 0, *b* 0.25, *c* 0.5, *d* 0.75, *e* 1.0, *f* 1.25, *g* 0.25, and *h* 1.0

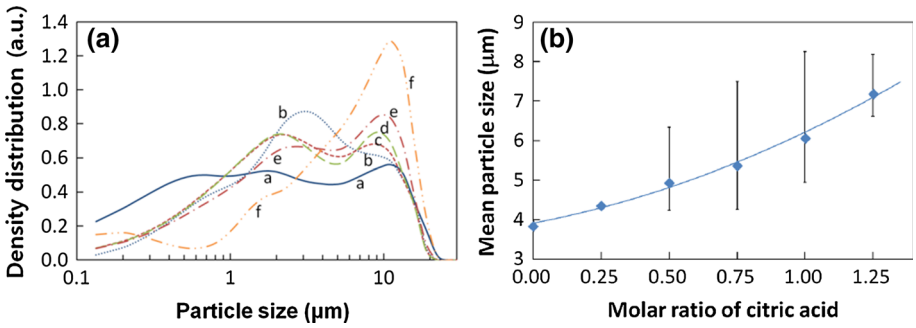

Fig. 6 Particle size distribution **a** and mean particle size **b** of Li_2MnSiO_4 as a function for molar ratio of citric acid

2.66–2.89, as calculated from the apparent intensity without the Gaussian deconvolution of the Raman spectra. This value is higher than that of graphite (1.58) and carbon black (2.00), meaning that the carbon formed on the Li_2MnSiO_4 particles is more amorphous.

SEM and TEM images of carbon-coated and noncoated Li_2MnSiO_4 particles are shown in Fig. 5. The Li_2MnSiO_4 without carbon, as shown in Fig. 5a, can be seen to consist of polygon-shaped particles with a submicron size. However, the primary particle size is dramatically reduced to below 100 nm in the case of the carbon-coated Li_2MnSiO_4, as shown in Fig. 5b–e. The TEM image of the carbon-coated Li_2MnSiO_4 synthesized using a citric acid to metal ion molar ratio of 1.0 in Fig. 5h reveals that this high concentration of citric acid causes carbon to be widely dispersed over the surface of the particle and create interconnections between particles. However, the particle synthesized from a low concentration of citric acid (a citric acid to metal molar ratio of 0.25) had only a tiny amount of carbon on its surface in the form of isolated islands, as shown in Fig. 5g. The particle size distribution shown in Fig. 6 reveals that the noncoated Li_2MSinO_4 has a very broad distribution ranging from 0.1 to 10 μm, and a mean particle size of 3.96 μm. With the addition of carbon, the particle size distribution becomes narrower, and there is an increase in the mean particle size due to secondary particles, even though it was confirmed by the SEM images that the size of the primary particles was reduced by carbon coating. The reason for this increase is believed to be that the coated carbon acts as an interconnecting material between particles [32].

Figure 7 shows the first and second charge–discharge profiles of non and carbon-coated Li_2MnSiO_4 electrodes at C/20 rate at 25 °C. In this figure, the noncoated Li_2MnSiO_4 shows a discharge capacity of around 3 mAh g^{-1}, which means no extraction and insertion of Li^+ ions from/into the structure. This is comparable with the work of Belharouak et al. who also observed a value of less than 10 mAh g^{-1} for Li_2MnSiO_4 without carbon coating [21]. When coated with 5.5 % carbon (equivalent to 0.5 mol of citric acid), the first and second discharge capacities were greatly improved to around 125 mAh g^{-1}. Indeed, this was true of most of the carbon-coated Li_2MnSiO_4 all of which exhibited a second discharge capacity of more than 100 mAh g^{-1} except for those coatings with less than 3 % carbon. Many researchers have reported a capacity of around 150 mAh g^{-1} at rate range of 0.02–0.05 C and a voltage range of 1.5–4.8 V for carbon-coated Li_2MnSiO_4 [13, 16, 21, 33, 34]. In this study, the carbon-coated Li_2MnSiO_4 delivered a slightly lower capacity because of the narrower voltage range used (2.0–4.7 V). Coulombic efficiency of the noncoated Li_2MnSiO_4 at first cycle was ca. 57 %, whereas the carbon-coated Li_2MnSiO_4 exhibited 76–81 % efficiency. Carbon coating led to a lowering of the irreversible reaction in the first cycle due to the reduced amount of impurities, with a subsequent increase in conductivity as shown in Figs. 1 and 2. As shown in Fig. 8, the capacities of all samples during cycling at C/5 rate continuously faded, which can be attributed to the structural change. Meanwhile, in Fig. 4, the nature of the carbon on Li_2MnSiO_4 can be seen to be very similar regardless of the amount of carbon coating. The electrochemical behaviors of the materials shown in Figs. 7 and 8 can therefore be attributed to the quantity of coated carbon, rather than its quality.

Figure 9 shows the variation in the second discharge capacity (initial capacity) at C/20 and the capacity fading rate for continuous cycling at C/5 for non and carbon-coated Li_2MnSiO_4 as a function of the carbon coating content, mean particle size, and electrical conductivity. We see from Fig. 9a that as more carbon is coated onto the particle, there is a linear increase in the initial capacity. Furthermore, the capacity fading rate also roughly increases with the carbon content. An increase in mean particle size, on the other hand, leads to an increase in the capacity and the fading rate, as shown in Fig. 9c, d, respectively. Even though the mean particle size increased with carbon coating, the decrease of the primary particle size was identified in the SEM images in Fig. 5. Therefore, the linear relationship between initial capacity and particle size

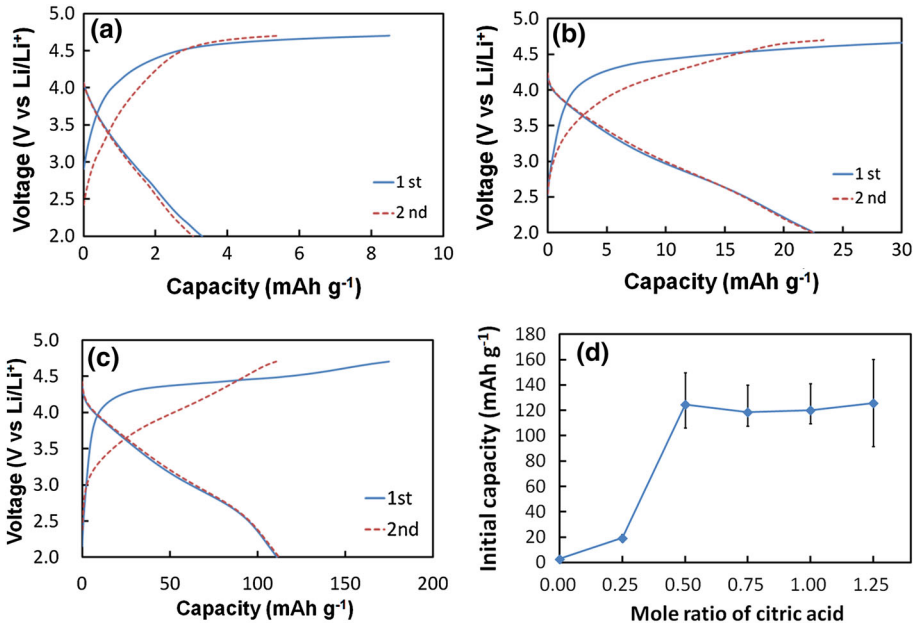

Fig. 7 Charge–discharge profiles and second discharge capacity of non and carbon-coated Li_2MnSiO_4 at C/20 rate as a function of molar ratio of citric acid. **a** 0, **b** 0.25, **c** 0.5, **d** 2nd discharge capacity

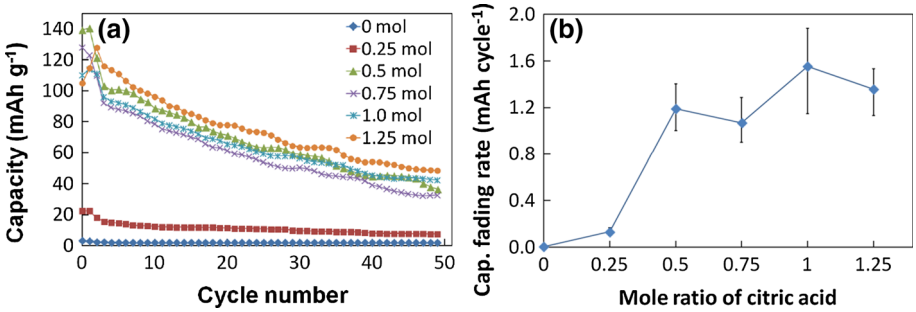

Fig. 8 Cycle performance **a** and capacity fading rate **b** of non and carbon-coated Li_2MnSiO_4 at C/5 rate as a function of molar ratio of citric acid

can be attributed to the decrease in primary particle size. The dependences of the electrical conductivity on capacity and fading rate show an exponential behavior in Fig. 9e, f. Dominko et al. found that the particles undergo a significant structural change to an amorphous phase after the first charge [15], and following subsequent discharge, the initial structure is not recovered. Furthermore, a decrease in the crystallinity of the powder by carbon coating was observed in the XRD patterns in Fig. 1. However, the R^2 values of the fitting in Fig. 9 match closely with the measured conductivity except in the case of the carbon coating and particle size. Those R^2 values for carbon coating and particle size are in the ranges of 0.64–0.69 and 0.49–0.54, respectively. It can therefore be concluded that the carbon coating leads to the decrease of the primary particle size and the improvement of electrical conductivity, and thus lithium ion can become easily accessible to particles. These lead to the increase of initial capacity of Li_2MnSiO_4. However, the capacity fading rate increases with the initial capacity because the change in the crystal structure of materials can be accelerated by the increase of capacity.

4 Conclusions

Carbon-coated Li_2MnSiO_4 powders were synthesized using a citric acid-assisted sol–gel process, by which the carbon content of the final powder could be easily controlled by varying the amount of citric acid added. Analysis of their charge–discharge characteristics in rechargeable lithium batteries using their physical properties revealed that this carbon coating altered the particle size distribution and electrical conductivity of the bulk materials, with a decrease in the level of impurities also detected by XRD. Furthermore, the carbon coating significantly increased the initial capacity of a Li_2MnSiO_4 powder with the discharge capacity of Li_2MnSiO_4 with a 5.5 % carbon coating ($\sim$125 mAh g^{-1}) representing a significant increase over the $\sim$3 mAh g^{-1} recorded for noncoated material. However, the discharge capacities of the carbon-coated materials during cycling at C/5 rate showed continuous fading. This can be attributed to a structural change to an amorphous phase, as well as the limitation of lithium ion diffusion that results from the material's low conductivity.

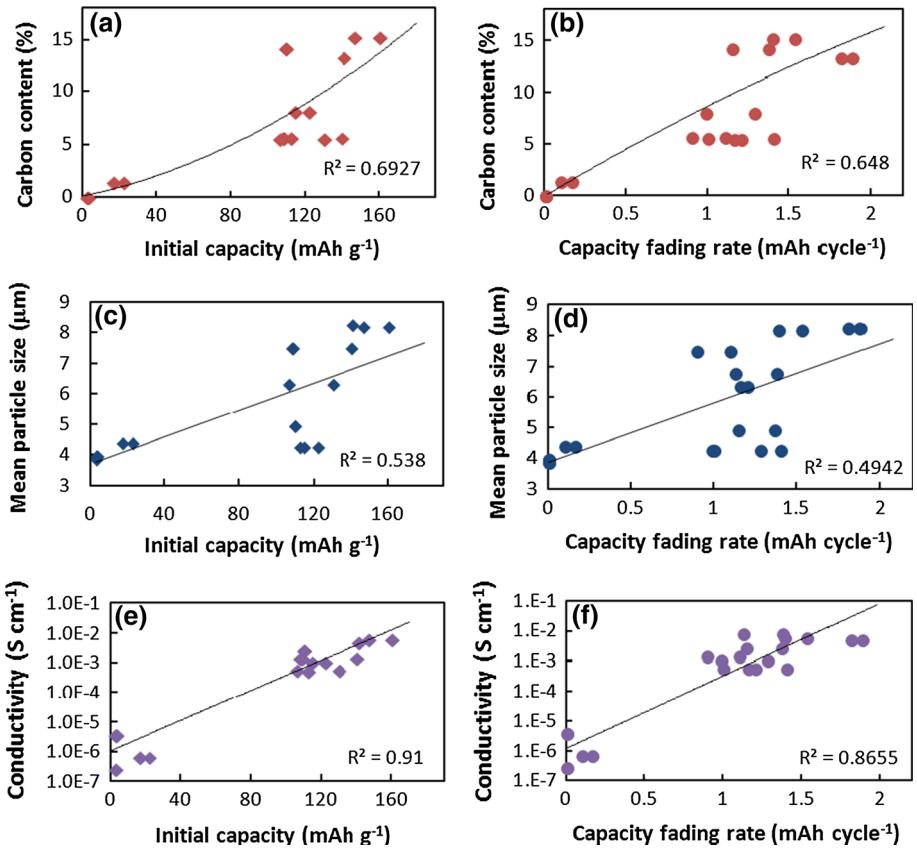

Fig. 9 Variation of second discharge capacities and capacity fading rates of non and carbon-coated Li_2MnSiO_4 according to carbon-coating content, mean particle size, and conductivity. **a**, **b** carbon content, **c**, **d** mean particle size and **e**, **f** conductivity

Acknowledgments This work was supported by the R&D Program through the National Fusion Research Institute of Korea (NFRI) funded by the government funds, and by the Degree & Research Center Program of the Korea Research Council of Fundamental Science and Technology.

References

1. Padhi AK, Nanjundaswamy AK, Masquelier C, Okada C, Goodenough JB (1997) Effect of structure on the Fe^{3+}/Fe^{2+} redox couple in iron phosphates. J Electrochem Soc 144:1609–1613
2. Padhi AK, Nanjundaswamy KS, Goodenough JB (1997) Phospho-olivines as positive-electrode materials for rechargeable lithium batteries. J Electrochem Soc 144:1188–1194
3. Padhi AK, Nanjundaswamy KS, Masquelier C, Goodenough JB (1997) Mapping of transition metal redox energies in phosphates with NASICON structure by lithium intercalation. J Electrochem Soc 144:2581–2586
4. Arroyo-deDompablo ME, Armand M, Tarascon JM, Amador U (2006) On-demand design of polyoxianionic cathode materials based on electronegativity correlations: an exploration of the Li2MSiO4 system (M = Fe, Mn Co, Ni). Electrochem Commun 8:1292–1298
5. Dominko R, Bele M, Gaberscek M, Meden A, Remskar M, Jamnik J (2006) Structure and electrochemical performance of Li_2MnSiO_4 and Li_2FeSiO_4 as potential Li-battery cathode materials. Electrochem. Commun 8:217–222
6. Aravindan V, Karthikeyan K, Kang KS, Yoon WS, Kim WS, Lee YS (2011) Influence of carbon towards improved lithium storage properties of Li_2MnSiO_4 cathodes. J Mater Chem 21:2470–2475
7. Dominko R (2008) Li_2MSiO_4 (M = Fe and/or Mn) cathode materials. J Power Sources 184:462–468
8. Tang XC, Li LX, Lai QL, Song XW, Jiang LH (2009) Investigation on diffusion behavior of Li^+ in $LiFePO_4$ by capacity intermittent titration technique (CITT). Electrochim Acta 54:2329–2334
9. Ravet N, Besner S, Simoneau M, Valee A, Armand M (1999) New electrode materials with high surface conductivity. CA 2270771 A1
10. Huang H, Yin SC, Nazar LF (2011) Approaching theoretical capacity of $LiFePO_4$ at room temperature at high rates. Electrochem Solid-State Lett 4:A170–A172
11. Prosini PP, Zane D, Pasquali M (2011) Improved electrochemical performance of a $LiFePO_4$-based composite cathode. Electrochim Acta 46:3517–3523
12. Gong ZL, Li YX, He GN, Li J, Yang Y (2008) Nanostructured Li_2FeSiO_4 electrode material synthesized through hydrothermal-assisted sol–gel process. Electrochem Solid State Lett 11:A60–A63
13. Aravindan V, Karthikeyan K, Amaresh S, Lee YS (2011) Superior lithium storage properties of carbon coated Li_2MnSiO_4 cathodes. Electrochem Solid-State Lett 14:A33–A35
14. Lv DP, Wen W, Huang XK, Bai JY, Mi JX, Wu SQ, Yang Y (2011) A novel Li_2FeSiO_4/C composite: synthesis, characterization and high storage capacity. J Mater Chem 21:9506–9512
15. Dominko R, Bele M, Kokalj A, Gaberscek M, Jamnik J (2010) Li_2MnSiO_4 as a potential Li-battery cathode material. J Power Sources 174:457–461
16. Deng C, Zhang S, Fu BL, Yang SY, Ma L (2010) Characterization of Li_2MnSiO_4 and Li_2FeSiO_4 cathode materials synthesized via a citric acid assisted sol–gel method. Mater Chem Phys 120:14–17

17. Zhang S, Deng C, Liu FL, Wu Q, Zhang M, Meng FL, Gao H (2013) Impacts of in situ carbon coating on the structural, morphological and electrochemical characteristics of Li_2MnSiO_4 prepared by a citric acid assisted sol–gel method. J Electroanal Chem 689:88–95
18. Arroyo-deDompablo ME, Amador U, Gallardo-Amores JM, Morán E, Ehrenberg H, Dupont L, Dominko R (2009) Polymorphs of Li_3PO_4 and Li_2MSiO_4 (M = Mn, Co): the role of pressure. J Power Sources 189:638–642
19. Gummow RJ, Sharma N, Peterson VK, He Y (2012) Crystal chemistry of the Pmnb polymorph of Li_2MnSiO_4. J Solid State Chem 188:32–37
20. Politaev VV, Petrenko AA, Nalbandyan VB, Medvedev BS, Shvetsova ES (2007) Crystal structure, phase relations and electrochemical properties of monoclinic Li_2MnSiO_4. J Solid State Chem 180:1045–1050
21. Belharouak I, Abouimrane A, Amine K (2009) Structural and electrochemical characterization of Li_2MnSiO_4 cathode material. J Phys Chem C 113:20733–20737
22. Kokalj A, Dominko R, Mali G, Meden A, Gaberscek A, Jamnik J (2007) Beyond one-electron reaction in Li cathode materials: designing $Li_2Mn_xFe_{1-x}SiO_4$. Chem Mater 19:3633–3640
23. Liu W, Xu Y, Yang R (2009) Synthesis, characterization and electrochemical performance of Li_2MnSiO_4/C cathode material by solid-state reaction. J Alloy Compd 480:L1–L4
24. Arroyo-deDompablo ME, Dominko R, Amores JMG, Dupont L, Mali G, Ehrenberg H, Jamnik J, Moran E (2008) On the energetic stability and electrochemistry of Li_2MnSiO_4 polymorphs. Chem Mater 20:5574–5584
25. Li YX, Gong ZL, Yang Y (2007) Synthesis and characterization of Li_2MnSiO_4/C nanocomposite cathode material for lithium ion batteries. J Power Sources 174:528–532
26. Muraliganth T, Stroukoff KR, Manthiram A (2010) On the energetic stability and electrochemistry of Li_2MnSiO_{-4} polymorphs. Chem Mater 22:5754–5761
27. Wyrzykowski D, Hebanowska E, Nowak-Wiczk G, Makowski M, Chmurzynski L (2011) Thermal behaviour of citric acid and isomeric aconitic acids. J Therm Anal Calorim 104:731–735
28. Bhuvaneswari MS, Bramnik NN, Ensling D, Ehrenberg H, Jaegermann W (2008) Synthesis and characterization of Carbon Nano Fiber/$LiFePO_4$ composites for Li-ion batteries. J Power Sources 180:553–560
29. Nagpure SC, Bhushan B, Babu SS (2012) Raman and NMR studies of aged $LiFePO_4$ cathode. Appl Surf Sci 259:49–54
30. Doeff MM, Wilcox JD, Kostecki R, Lau G (2006) Optimization of carbon coatings on $LiFePO_4$. J Power Sources 163:180–184
31. Zaghib K, Ait Salah A, Ravet N, Mauger A, Gendron F, Julien CM (2006) Structural, magnetic and electrochemical properties of lithium iron orthosilicate. J Power Sources 160:1381–1386
32. Oh SW, Myung ST, Oh SM, Oh KH, Amine K, Scrosati B, Sun YK (2010) Double carbon coating of $LiFePO_4$ as high rate electrode for rechargeable lithium batteries. Adv Mater 22:4842–4845
33. Deng C, Sun YH, Zhang S, Lin HM, Gao Y, Wu B, Ma L, Shang Y, Dong G (2012) Synthesis and improved properties of nanostructured Li_2MnSiO_4/C via a modified sol–gel method. Int J Electrochem Sci 7:4559–4566
34. Zhang S, Deng C, Gao H, Meng FL, Zhang M (2013) $Li_{2+x-}Mn_{1-x}P_xSi_{1-x}O_4$/C as novel cathode materials for lithium ion batteries. Electrochim Acta 107:406–412